Mem. S.A.It. Vol. 74, 815

Memorie della

Characterization of the IBIS Transmission Profile

K. Reardon and F. Cavallini

INAF/Osservatorio Astrofisico di Arcetri

Abstract. We describe the techniques used to characterize the components of the IBIS instrument in the laboratory in order to determine the operational performance of the completed instrument. In particular, we have measured the surface and coating irregularities of the two Fabry-Perot interferometers at the heart of IBIS. From this we construct a theoretical transmission profile for the instrument and relate that to the accuracy that can be obtained in measurements of the Sun.

Key words. Inteferometers, Instrumentation

1. Introduction

IBIS is a dual Fabry-Perot interferometer instrument (Cavallini et al., 2003) that uses two complementary air-spaced interferometers to select narrow wavelength bands in the solar spectrum. The two interferometers can simultaneously adjust their spacing in a coordinated manner in order to tune through a range of wavelengths, maintaining both spectral purity and high transmission over this range. Dual interferometers offer the advantage of a high throughput, allowing rapid acquisition of a complete data cube $\{x, y, \lambda\}$.

However, the performance of any such instrument is strongly dependent on the particular characteristics of the interferometers utilized. The system performance derived during the design stage are based on certain assumptions and simplifications concerning the characteristics of the interferometers (see Table 1). However, the true characteristics, including both mean values and distributions of certain parameters, may strongly influence the generated instrumental profile. In particular, the distribution in the figure errors of the plates of a Fabry-Perot, and hence variations in spacing between the two plates, is often assumed to have a gaussian or other analytical distribution, yet such an assumption may not be valid for all interferometers. We have therefore performed a set of measurements in order to characterize the Fabry-Perot's used in the IBIS instrument.

	F-P #1	**F-P #2**
Plate Separation	2.3 mm	0.66 mm
Plate Flatness	λ / 150	λ / 150
Reflectivity	0.94	0.94
FWHM	22.6 mÅ	78.4 mÅ
Absorbtion	0.002	0.002

Table 1. *Nominal characteristics of the two IBIS Fabry-Perot interferometers (at 632.8 nm)*

Send offprint requests to: K. Reardon, kreardon@arcetri.astro.it

2. Measurements

A single-mode HeNe laser ($\lambda = 632.817$ nm) was used to illuminate the plates of each interferometer individually. The plate spacing was tuned through the wavelength of the laser in 1.325 mÅ and 4.61 mÅ steps for FP #1 and #2 respectively. At each spacing step, spatially resolved images of the transmission were obtained with a 12-bit CCD camera. The data were obtained in multiple configurations with a resolution of approximately 30 microns across the plates of the Fabry-Perot. The full aperture of the interferometers is 50 mm for both, though only approximately 46 mm was illuminated in these tests. The laser's narrow emission profile ($\approx$ 1 mÅ) was sufficiently fine to fully resolve the transmission profile of the interferometers.

From the observed transmission profile at each point on the interferometer, the profile width (FWHM) and peak shift were measured. From this the plate spacing and reflectance at that location could be determined according to the following formulae:

Plate Separation:

$$\Delta \text{ d} / \text{d} = \Delta \lambda / \lambda_o$$

Reflectance:

$$\text{FWHM} = \lambda_o * (1 - R)/(2\pi d\sqrt{R})$$

where d is the nominal separation, λ_o the measurement wavelength (632.8 nm), and R the nominal reflectance.

Using this technique, we constructed maps of the cavity errors (Figure 1) and reflectance (Figure 2) across the interferometer surfaces. We see from these maps that the errors in reflectivity (due to irregularities in the coatings applied to the interferometer plates) are essentially randomly distributed. The surface errors, beyond a general pattern of errors, show both localized errors due to small plate defects (black "dots" in Figure 1), as well a large scale increase in the plate separation towards the edge of the interferometers. The small scale defects were generally present on one interferometer, while the *bowing* of the Fabry-Perot plates was present for both. Table 2 gives the average measured quantities for the two Fabry-Perot interferometers.

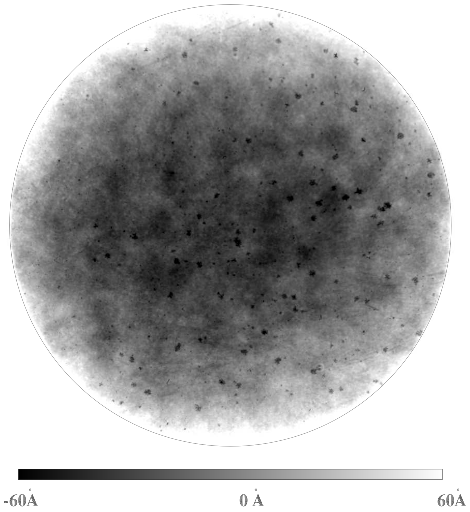

Fig. 1. Cavity errors of Fabry-Perot #1 relative to the mean spacing, in Å.

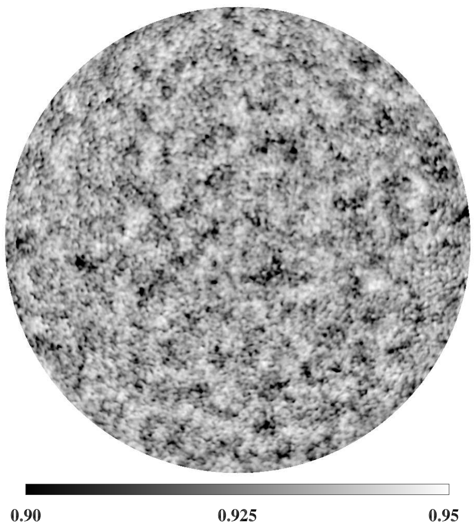

Fig. 2. Reflectivity of Fabry-Perot #1.

	F-P #1	F-P #2
Flatness	-40,+140 mÅ	-40,+110 mÅ
Reflectivity	0.923	0.916
FWHM	22.1 mÅ	85.2 mÅ
Absorbtion	0.005	0.005

Table 2. *Measured Fabry-Perot characteristics at 632.8 nm*

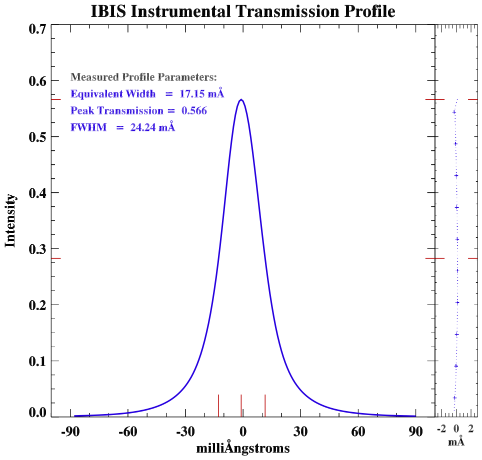

Fig. 3. Overall instrumental profile of the dual interferometers.

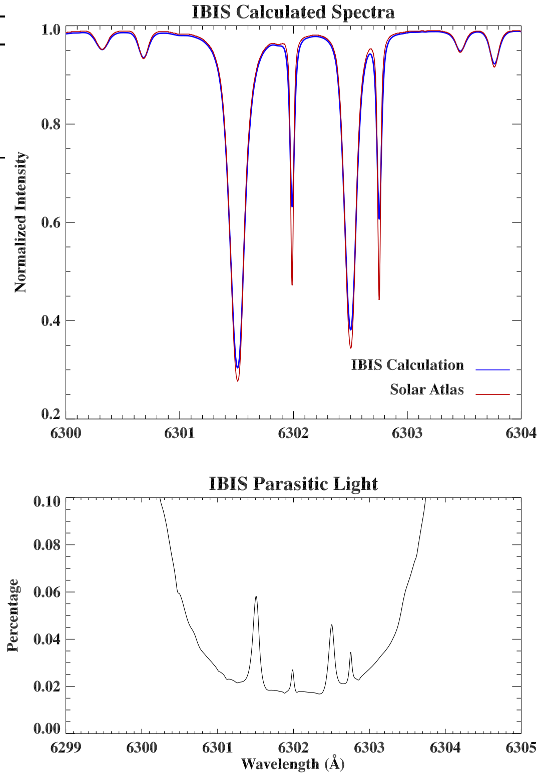

Fig. 4. (a) Calculated IBIS spectrum as compared with solar atlas; (b) Parasitic light present in the spectrum, relative to the intensity at each spectral point.

3. Instrumental Profile

We were able to obtain a map of the cavity errors over a 46 mm diameter area of the 50 mm Fabry-Perot by measuring the shift of the profile at each point. Using a subaperture of the interferometer (30 mm diameter), we also derived a reflective profile in which the only remaining errors are those caused by variations in reflectivity across the interferometer. This was done by aligning the individual profiles to a common peak position, removing any shifts caused by spacing errors. By convolving the distribution of cavity errors measured over a given area with the observed reflective profile, we can then construct the expected instrumental transmission profile for any aperture.

For an instrument using the classical mounting of the interferometers, such as IBIS, each observed spatial point integrates equally over the illuminated interferometer aperture. Different configurations of the instrument will result in different illumination of the interferometers, and hence the overall profile will be dependent on total area illuminated (e.g. 35 mm at the Dunn Solar Telescope; 39 mm at THEMIS).

Due to the observed curvature in the plate separation from the center to edge, enlarging the aperture results in an increasing asymmetry of the instrumental transmission profile, so that apertures above approximately 40 mm are probably not usable with these Fabry-Perot interferometers in a classical mounting configuration. Alternatively, in a telecentric mounting, this curvature would produce a secondary wavelength shift across the field of view.

We then fit a theoretical Airy function to the observed reflective profile in order to determine the transmission at points in the minima between the interferometer transmission peaks. This allows us to construct the complete instrumental profile over the entire significant range of instrument transmission, as determined by the prefilter passband (Figure 3). From this, it is possible to calculate the "parasitic light" of the instrument, the percentage of transmission falling outside of the primary peak. Finally, by convolving the complete instrumental profile, consisting of the combination of the two Fabry-Perot interferometers and a prefilter, with a solar spectral atlas, we can determine the shape of the observed solar spectral lines with IBIS. This is shown in Figure 4 for the spectral lines at 6302 Å and a fixed prefilter passband (3 Å FWHM). The parasitic light is determined at each point in the spectrum, comparing the overall flux in the central peak of the convolved profile, with the flux outside that peak.

References

Cavallini, F., Baffa, C., Reardon, K., Berrilli, F., Cantarano, S., Egidi, A.: 2003, *this volume*